Accepted for publication in the AIAA Journal on 14th August 2019

Experimental and Theoretical Verification of the Frozen Sonic Flow Method for Mixtures of Polyatomic Gases

A. Esposito[1]
University of Naples "Federico II", Naples, Italy, 80125

M. Lappa[2]
University of Strathclyde, Glasgow, UK, G1 1XJ

Abstract: A contemporary issue of crucial importance for further developments in the field of thermal protection systems and related arc-jet-based testing activities calls for improvements in existing abilities to measure the centerline total enthalpy. Starting from the original assumptions of Vincenti and Kruger (1965) and through the elaboration of a mathematical framework relying on a specific modelling hierarchy of balance equations for the moles of different species involved, we show that the extension of the Frozen Sonic Flow Method (FSFM) to the case of polyatomic molecules can be made well posed. Dedicated experiments have been conducted using a re-entry simulation facility and varying the mass-averaged enthalpy in the range between 5 and 30 [MJ/kg]. In particular, three different gas mixtures have been considered (using Nitrogen as hot feeding gas and adding cold Oxygen, Carbon Dioxide and Methane, respectively). The enthalpy ratios calculated by the FSFM, found to depend on the gas mixture, have been compared with the values determined using two alternate techniques, namely, 1) the Heating Rate Method and 2) the Calorimetric Probe Method. Given the extremely complex experimental conditions considered (high-enthalpy, low density, supersonic reactive flows), the agreement between the theoretical and experimental results can be considered very satisfactory.

Key words: arc-jet facility, center-line enthalpy, Frozen Sonic Flow, Polyatomic Gas Mixtures

[1] PhD in Aerospace Engineering, Lab Head, *Department of Industrial Engineering, Via Claudio 21, email: antespos@unina.it*
[2] PhD in Aerospace Engineering, Director of the Advanced Course (MSc) in Mechanical Engineering, *Department of Mechanical and Aerospace Engineering, James Weir Building, 75 Montrose Street, email: marcello.lappa@strath.ac.uk*

Nomenclature

A^* = cross-sectional area of nozzle throat (m^2)

C_p = specific heat

c_i = mass fraction of the i^{th} species

h_d^0 = dissociation energy MJ/kg

F = gamma function

H = total enthalpy (MJ/kg)

H_T = heat content at temperature T, (MJ/kg)

K = constant in eq. (29 a)

k_w = catalytic reaction rate constant (m/s)

Le = Lewis number

m_g = gas mass flow rate (kg/s)

m_0 = molecular mass of undissociated gas (kg/kmoles)

n = number of moles

p = pressure (Pa)

P = electrical power (kW)

q = heat flux (kW/m^2)

R = body nose radius (m)

R_0 = universal gas constant (J/kmoles/K)

Sc = Schmidt number

T = temperature (K)

n_i^* = molar fraction of the i^{th} species

Z = compressibility factor

$\Delta H_{f,T}$ = heat of formation at temperature T (MJ/kg)

ρ = density kg/m^3

η = catalytic efficiency

ζ = corrective factor for the Vincenti and Kruger formula

ψ = number of atoms contributing to the formation of new polyatomic species

χ = number of atoms produced by the dissociation of each polyatomic molecule

ξ = ratio of moles of polyatomic and diatomic gas in the initial state

α = total mass fraction of dissociated species

μ = viscosity (kg/ms)

γ = isentropic exponent

Subscripts

ψ = new polyatomic species not present in the reference state

ah = arc-heater

cl = nozzle centerline

d = diatomic

e = boundary layer edge

g = gas

H2O = water

m = monoatomic

mc = mixing chamber

ne = nozzle exit

p = polyatomic

t = total condition (at the beginning of expansion)

ts = test section

w = wall

Superscripts

0 = reference state (undissociated gas)

A = undissociated diatomic gas present in the final state

B = diatomic gas originating from the dissociation of polyatomic gas

I. Introduction

Complex fluid flow and heat transfer problems are central to many advanced aerospace systems often at the cutting-edge of modern engineering. This is indeed the case of re-entry space vehicles, which require a detailed understanding of the overall aero-thermodynamic behavior, including (but not limited to) the distribution of pressure, heat flux, and enthalpy. Reliable estimates of such quantities (or high-resolution measurements) are typically needed for the proper design and performance assessment of related protection systems (De Filippis et al., [1,2]; Zare-Behtash et al. [3,4]). During the re-entry phase, critical or "delicate" vehicle parts such as the nose, the leading edge of wings and/or the flaps are subjected to very high temperatures and stresses and would degrade quickly if not designed properly to resist high thermal and/or mechanical loads.

Such problems are generally handled in the framework of on-the-ground testing activities, based on arc-jet facilities typically used for the qualification of such thermal protection systems (TPS) (Balboni [5]; Esposito et al. [6]; Zuppardi and Esposito [7,8] Esposito et al. [9]; Venkatapathy et al. [10]). The key point with which engineers have often to deal with in such a context is represented by the need to mimic effective flight conditions with a reasonable approximation. This, in turn, implies the ability to "control" with a sufficient degree of accuracy the conditions effectively attained inside these facilities.

This objective can reasonably be met if the attempt to measure or control precisely the different quantities discussed before is limited to one or two of them. Usually the parameter of major concern or interest is represented by the *heat flux* given the crucial role it can play in determining the response of a vehicle (or one of its components) to the effective flight conditions. However, also the *enthalpy* has to be seen as a very important influential factor. In many circumstances, indeed, the fluid displays a complex chemical composition essentially depending on this parameter.

Though measuring the enthalpy relating to an arc-jet facility is not straightforward as one would imagine (Suess et al. [11]), estimates can be obtained using different strategies such as the sonic throat method (Winovich [12]) and the energy balance approach [13].

These methods generally share a common feature, that is, they rely on the approximation that the enthalpy can be treated as an average quantity over the entire flow field. This, however, should be seen as a crude simplification. The enthalpy is indeed known to display a complex spatial distribution, varying significantly along the radial extension of the facility due to heat loss through its external boundary and/or according to the specific technical solution implemented to generate the arc.

Leaving aside for a while the effects of the specific geometry considered, in general, enthalpy in the test section of an arc-jet facility typically attains it highest value at the center-line, and then decreases towards the nozzle walls. The aforementioned tests aimed to assess the performances of TPS are usually conducted in the inner or "core" region. The enthalpy of the core is generally referred to as "center-line" enthalpy; as the reader will have realized at this stage, this is the value to be made as close as possible to the flight value.

Along these lines, over the years a number of possible strategies to determine this quantity have been elaborated and in the future, undoubtedly, more exciting activity in this area will be stimulated (the present work being an attempt in this direction). Most of the existing approaches have been based on a common pre-conception, that is, the ratio of the center-line to bulk enthalpy can be determined as a function of other parameters. In practice, such a ratio can depend in a relatively complex way on many different influential factors, these being the physical geometry of the heater, the air injection mode into the heater, the gas mass flow rate, the electrode configuration, the presence or absence of mixed gases, the geometry of the mixing chamber, the nozzle configuration, etc. From a purely theoretical standpoint, however, there is some consensus in the literature that a proper characterization of this ratio can be based on a handful of *specific measurements* and *adequate mathematical models*.

Indeed, one of the proposed strategies, known as "sonic flow method", relies on the original idea proposed by Winovich [12] that the centerline enthalpy in arc-heated flows originating from high pressure reservoirs (i.e. from an equilibrium state), can be determined assuming that the conditions at the sonic point of the nozzle correspond to a one-dimensional, isentropic expansion in equilibrium conditions. The method was extended by Jorgensen [14], who successfully applied it to flows that are in equilibrium through a reservoir up to the beginning of expansion and suddenly freeze at that point (the so-called "frozen sonic point method"). Finally, Pope [15] verified the reliability of this approach for high-enthalpy flows which freeze upstream the beginning of expansion, the only pre-requisite to its applicability being represented by proper knowledge of the chemical composition of the frozen flow. Other techniques have also been elaborated such as that described by Hiester and Clark [16], based on center-line measurements of the stagnation point heat flux and pressure used together with a heat flux prediction correlation such as that provided by the Fay and Riddell theory (the reader being also referred to Zhang et al. [17]).

In such a context, the experimental parameters to be used as inputs for the application of these methods have been determined using various techniques such as spectroscopic and laser scattering methods, energy balance

probes, and laser induced fluorescence (LIF) (see, e.g., Scott [18] and Park [19] for exhaustive reviews and Suess et al. [11] for valuable recent findings, respectively).

By examining such material, the reader will realize that work in these fields has progressed with the aid and support of experimental results used in synergy with theoretical models to improve the representation of the thermofluid-dynamic processes inside arc-jet facilities, moving through very focused examples and situations, many of which of a prototypical nature (Park [19]; Esposito et al. [20], Lappa [21]).

As the interplay between experimental measurements and analytic arguments has been particularly fruitful, new efforts have recently been devoted to explore the response of these methods in circumstances for which their pre-requisites were thought not to be valid or weak. An example along these lines is represented by the recent attempt by Esposito and Aponte [22] to extend the frozen sonic point technique to polyatomic molecules gas mixtures. These efforts and synergy with experimental work have led over the years to the establishment of a common, elegant theoretical framework based on the original theory for di-atomic molecules elaborated by Vincenti and Kruger [23] and Chapman and Cowling [24]. Building on such track of results, the present work continues this line of inquiry by probing the role of polyatomic molecules.

An extension of the ranges of applicability of these techniques is likely to yield important benefits, for example, better process control, increased efficiency, improved reproducibility and the capacity to modify or tailor arc-jet facilities for specific applications.

The present paper is articulated into several sections. In Section II, we describe in a schematic way the facilities and instruments used to conduct the experiments. Section III is entirely devoted to a presentation of the methodological approach and related variants (part of the role of this section is the review of concepts that will be applied in later sections). In particular, while Sect. III.A is used to introduce the energy balance method and related governing equations, the Frozen Sonic Flow Method (FSFM) is treated in Sect. III.B (where the related underlying hypotheses are critically discussed together with the necessary pre-requisites for applicability; however, no assumptions are made at this stage on the nature of the gas). The general foundations of our theoretical treatment of polyatomic gases are laid in the following section (Sect. III.C) through a precise hierarchy of balance equations (in terms of gas moles) for the different species present in the initial (reference) and dissociated states. This modus operandi finally leads to generalized formulas (with respect to those originally introduced by Vincenti and Kruger [23]) for the compressibility factor and isentropic exponent (γ) required for the application of the FSFM. Other experimental methods to be used for an evaluation of the centerline enthalpy are dealt with in Sect. III.D. These methods are the Heating Rate Method (HRM) and the

Calorimetric Probe Method (CPM). As the reader may have realized at this stage, these methods are used to obtain independent measurements used to demonstrate the reliability and accuracy of the overall approach (cross comparison of all these values naturally leads to reciprocal validation of alternate strategies for the derivation of the enthalpy). All the results are finally used to populate Sect. IV, where, in order to improve the manuscript readability, the findings obtained with different methods are combined in a series of representative plots. As discussed in more detail in the conclusions section, the final outcome is a generalized theoretical-experimental framework incorporating the capacity to deal with an extended set of circumstances.

II. Experimental Apparatus (Facilities and Instruments)

The hardware used for the effective experiment executions and related measurements can shortly be described as follows:

A. The Small Planetary Entry Simulator

The test campaign has been based on the arc-jet facility SPES (Small Planetary Entry Simulator) Esposito and Aponte [22] (Fig.1a). The SPES is a continuous, open circuit arc-driven facility. In a continuous wind tunnel like this the gas flow is processed with no practical limitations on the run time; this characteristic of the SPES (its main components being shown in Fig.1b) may be regarded as a distinguishing mark with respect to other categories of devices such as intermittent wind tunnels where the gas flow is produced by rapid discharge of a high-pressure storage tank or suction from an evacuated reservoir (in these cases the run time is limited by the considered tank or reservoir capacity) :

1. Gas feeding system (typical total mass flow rates are between 0,5 and 1 g/s)
2. Electric arc-heater (industrial plasma torch, Sulzer-Metco 9-MB, with arc swirl stabilization), operating with pure inert gases (normally nitrogen but also argon, helium and their mixtures can be used) at maximum power of 60 [kW]
3. Mixing chamber (swirl mixer) where cold gases (oxygen, carbon dioxide and others) can be added to the plasma gas to create gas mixtures
4. Conical nozzles with different area ratios (4, 20, 56) for operations in supersonic and hypersonic regimes (the nominal values of the Mach number corresponding to such ratios for γ=1.4 being 2.94, 4.72 and 6.05, respectively; Flow Run Time for SPES being ‘continuous’, as explained above).
5. Cylindrical test chamber

6. Diffuser comprising 3 stages or parts
7. Heat exchanger
8. Vacuum system (capable of minimum pressure of 50 [Pa] in the test chamber)
9. Exhaust (open air, after gas purification)

a)

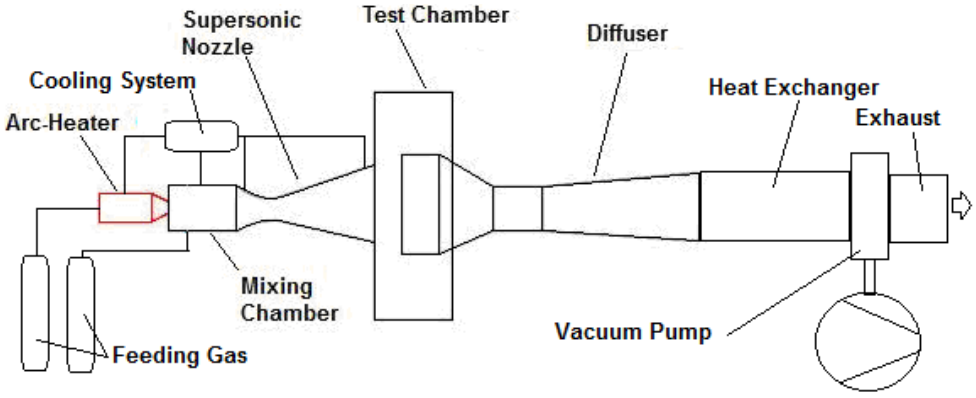

b)

Figure 1. Small Planetary Entry Simulator (SPES): (a) overall picture, (b) layout

B. Instrumentation

The feeding gas mass flow rates have been measured by thermal mass flow-meters while the nozzle and torch cooling water flow rates have been measured by variable-area flow-meters. Arc-heater Electrical parameters have been measured by digital instruments with data acquisition relying on a dedicated digital system able to measure and store the thermocouple temperatures located all along the components. Pressure measurements

have been made by absolute transducers calibrated by a capacitive vacuum gauge. The uncertainty on the measured pressures (vacuum capacitive transducers), temperatures (thermocouples) and mass flow rates (mass flow meters) was 2-5%, 7-10%, 3-5%, respectively.

III. Methods

A. Averaged Total Enthalpy Measurement

In our experiments, the bulk enthalpy (H_{ne}) has been determined at three different positions along the SPES (Refer to Fig. 1) by the *so-called energy balance method* (see, e.g., Pope [15]).

In particular, the measured enthalpies have been calculated as average values resulting from different energy contributors at each position, as illustrated in the following:

i) The enthalpy of the gas leaving the arc-heater and entering the mixer:

$$H_{ah} = \frac{P - (m_{H2O} C \Delta T)_{\mathrm{ah}}}{m_{g,ah}} \tag{1}$$

(evaluated by subtracting the losses due to the cooling water to the input electric power and assuming C=4186 [J/kgK], the reader being referred to the nomenclature for the meaning of symbols)

ii) The enthalpy of the gas leaving the mixer and entering the nozzle:

$$H_{mc} = \frac{\mathrm{H_{ah}m_{ah}} - (m_{H2O} C \Delta T)_{\mathrm{mc}}}{m_{g,t}} \tag{2}$$

iii) The enthalpy of the flow at the nozzle exit:

$$H_{ne} = H_{mc} - \frac{(m_{H2O} C \Delta T)_{ne}}{m_{g,t}} \tag{3}$$

During each test the following pressures have been measured by electronic vacuum transducers:

- p_t , at the mixing chamber exit
- p_{ne} , at the nozzle exit
- p_{ts} , at the test section
- p_{02} , impact pressure at the stream centerline.

The uncertainty on the measured total enthalpy H_{ne} was in the range between ±10% and ±20% depending on arc power level, while the overall repeatability of the SPES for the present tests was ≅ 95% (according to our experience, such repeatability decreases as some specific parts of the arc-heater are consumed).

B. The Frozen Sonic Flow Method (FSFM)

As stated in the introduction, the method of primary interest to be used in determining the total enthalpy is the so-called FSFM. This method was originally introduced for flows that, starting from the sonic point of the supersonic nozzle (refer again to Fig. 1), can be represented by a one-dimensional, isentropic expansion in equilibrium conditions. Jorgensen [14] extended it to the case in which flows that are in equilibrium through a reservoir up to the beginning of expansion, suddenly freeze at that point (in line with widespread consensus in the literature that if the pressure is sufficiently small, the flow can be assumed to freeze quickly once it departs from equilibrium, Cheng and Lee [25]). Following Jorgensen [14], the equation for frozen expansion, allowing the evaluation of total temperature (T_t) at the beginning of the expansion, simply reads:

$$m_g/p_tA^*=CF(\gamma)/(ZT_t)^{1/2} \tag{4}$$

where m_g and p_t are measured during the test, A^* is the sonic section and Z is the so-called compressibility factor; moreover,

$$C = m_0 / R_0 \tag{5}$$

$$F(\gamma) = [\gamma(2/\gamma+1)^{(\gamma+1)/(\gamma-1)}]^{1/2} \tag{6}$$

where γ is the isentropic exponent. In principle, this parameter must be evaluated for a chemically frozen mixture of atomic, diatomic and polyatomic species, with frozen vibrational energy *using the chemical gas*

composition (c_i) determined by the knowledge of enthalpy and pressure at the arc-heater exit. In reality, this specific stage is not as straightforward as one would imagine and requires additional details and explanations.

In practice, in order to apply the FSF method, the thermo-chemical state of the gas must be evaluated at certain important sections along the arc-jet process, namely, (a) at the arc-heater exit; (b) at mixing chamber, just downstream the cold gas injection point; (c) at the nozzle exit.

In particular, the following three subsequent steps have to be implemented:

1) From the energy-balance measurements illustrated in Sect. III.A, the bulk enthalpies H_{ah}, H_{mc}, H_{ne} at the stations (a), (b) and (c) are determined.

2) Owing to the small value of the arc-heater pressure (3.0×10^4 [Pa] in the present work), the gas flow at the arc-heater exit can be assumed to be in thermo-chemical equilibrium (Brown [26]); measuring the pressure and knowing H_{ah}, the gas temperature and chemical composition can be determined using the data reported by Gross et al. [27] (see their Figs. 58 and 68, which provide the temperature vs enthalpy, and the concentration of atomic nitrogen vs the temperature, respectively).

3) The chemical composition in the mixer chamber, just downstream the cold gas injection point (i.e. the freezing point) is evaluated by means of the on-line CEA code from NASA (Sanford and McBride [28]), using the Nitrogen plasma coming from the torch and the cold gas injected into the mixer as starting data. This procedure assumes that chemical reactions occur instantaneously within an adiabatic process. Once the composition of the gas is computed by CEA, we then calculate the compressibility factor Z and the specific heat ratio γ (further details being given in Sect. III.C) and the total temperature T_t (via eq. (4)).

Once T_t is known, using the chemical composition derived from the JANAF thermo-chemical data (Stull et al. [29]; see also www.kinetics.nist.gov/janaf/), the centerline enthalpy can finally be calculated as:

$$H_{CL}=\Sigma c_i\,(H_T+\Delta H_{f,T})_i \tag{7}$$

To simplify the data reduction, in general, the values of $(H_T+\Delta H_{f,T})_i$ are correlated in terms of temperature, i.e.:

$$(H_T+\Delta H_{f,T})_i=B_1T+B_2 \tag{8}$$

It is hardly worth noting that among the JANAF curves related to the chemical species used in the present FSF method, only CO and CO_2 species have a negative term (HT + ΔHf,T) for almost temperatures as shown in Fig. 2.

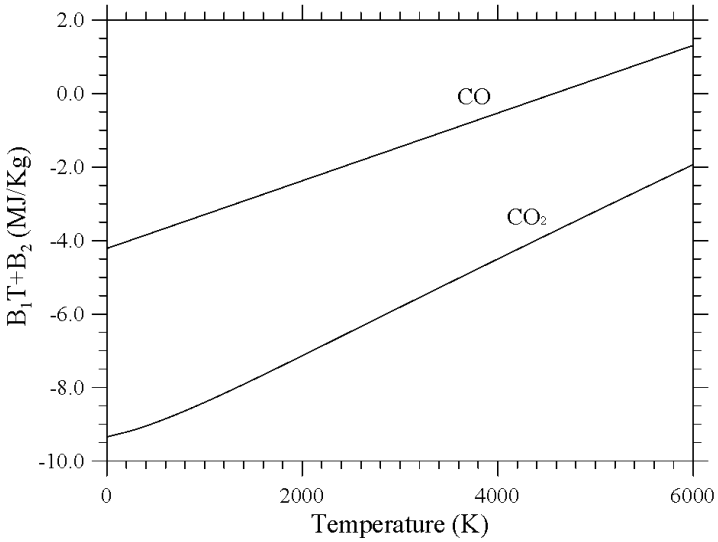

Figure 2. JANAF (1998 edition) curves for CO and CO_2

C. Extending the Vincenti and Kruger Formula

As we have illustrated in the preceding section, the frozen sonic flow method largely relies on the so-called compressibility factor and the corresponding value of γ (namely the ratio of the specific heat coefficients at constant pressure and volume). In this section, we therefore lay the foundations of a possible *extension* of the approach originally elaborated by Vincenti and Kruger [23] to the case of a mixture of partially (or completely) dissociated gases.

Vincenti and Kruger [23] developed a specific mathematical model under the assumption that, after the dissociation process, the gas composition is fixed at same value and the vibrational degree of freedom is frozen. Still retaining the same assumptions, we target an extension of such model to the more general situation in which the mixture of gases before the dissociation process also includes polyatomic species (a mixture of N_2 and CO_2 or CH_4) and species of such a kind are even present in the dissociated state, e.g. HCN (in [23], the theoretical framework was limited to the case of initial diatomic and symmetrical gases only, namely, O_2 and N_2, i.e. the main components of air). Along these lines, we start from the simple remark that the simple expression for the compressibility factor

$$Z_{VK} = 1 + \alpha \tag{9}$$

determined by these authors (and extensively used by many researchers, where α is the mass fraction of dissociated gas, see, e.g., Pope [15]), *should not be used* when polyatomic species are involved as it heavily relies on the aforementioned assumptions in terms of gas molecular structure. Therefore, we develop our revised approach on the basis of the original definition of the compressibility factor, which, as reported in Vincenti and Kruger [23], can formally be expressed as

$$Z = \frac{n}{n^0} \tag{10}$$

where n represents the total number of moles in the dissociated gas mixture while n^0 accounts for the corresponding number in the initial (non-dissociated) state. In the following, in particular, we denote the number of moles of diatomic and polyatomic species present in the initial state by n_d^0 and n_p^0, respectively:

$$n^0 = n_d^0 + n_p^0 \tag{11}$$

Starting from these premises, and following the same strategy implemented by Vincenti and Kruger [23], a relevant framework for the determination of the quantity γ can be built by defining proper balance equations (in terms of gas moles) for the different species present in the initial (reference) and dissociated states.

The first logical step in this modelling hierarchy obviously relates to considering the monoatomic species present in the final dissociated state. Due to the dissociation of diatomic species, in the final state there will be a number of moles of monoatomic species $2\left(n_d^0 - n_d^A\right)$ where n_d^A is the number of moles of diatomic species which have survived the dissociation process. In our case, however, also the polyatomic species can give rise to some monoatomic species; for this reason, there will also be a contribution $\chi\left(n_p^0 - n_p\right)$ where χ is the number of atoms produced by the dissociation of each polyatomic molecule. The balance equation for the monoatomic species (n_m) can therefore be formulated as

$$2\left(n_d^0 - n_d^A\right) + \chi\left(n_p^0 - n_p\right) = n_m + \psi n_\psi \text{ (balance for the monoatomic species)} \quad (12)$$

where ψ is the number of atoms contributing to the formation of new polyatomic species (e.g., HNC for the case of CH_4) in the final state (and n_ψ accounts for the related number of moles).

Accordingly, the number of moles in the final state for the diatomic species will read:

$$n_d = n_d^A + n_d^B \quad (13)$$

where the A superscript represents diatomic gas in the final state due to diatomic gas present in the initial state, which has not undergone dissociation and the B superscript represents diatomic gas originating from the dissociation of polyatomic gas (we assume that each molecule of polyatomic gas can give rise to one molecule only of diatomic gas, which is indeed the case of both CO_2 and CH_4), i.e.

$$n_d^B = n_p^0 - n_p \text{ (balance for dissociation of polyatomic species)} \quad (14)$$

From a global point of view, moreover, the following balance equations shall also be satisfied:

$$n = n_m + n_d + n_p + n_\psi \text{ (global balance)} \quad (15)$$

We assume

$$\chi = \begin{cases} 1 \ for \ CO_2 \\ 3 \ for \ CH_4 \end{cases} \quad (16)$$

This assumption being justified by the observation that CO_2 simply dissociates in CO and O, while each molecule of CH_4 gives rise to a molecule of H_2, two atoms of H and one atom of C. Moreover,

$$\psi = \begin{cases} 0 \ for \ CO_2 \\ 3 \ for \ CH_4 \end{cases} \quad (17)$$

as no polyatomic specie is formed when a mixture of N_2 and CO_2 is considered, whereas a mixture of N_2 and CH_4 can give rise to a significant percentage of HCN.

Expressing all quantities as a function of n_d and n_d^0 leads to:

$$n_p = n_p^0 - n_d^B \tag{18a}$$

$$n_m = 2\left(n_d^0 - n_d^A\right) + \chi n_d^B - \psi n_\psi \tag{18b}$$

$$n_m = n - \left(n_d^A + n_d^B\right) - n_p^0 + n_d^B - n_\psi = n - n_d^A - n_p^0 - n_\psi \tag{18c}$$

Imposing that the right-hand side of eq. (18b) and (18c) are equal, one gets:

$$\chi n_d^B - n_d^A = n - 2n_d^0 - n_p^0 + \left(\psi - 1\right) n_\psi \tag{19}$$

Expressing all quantities as a function of n_p, after some manipulations, the system of independent equations can also be rewritten as

$$n_d^B = n_p^0 - n_p \tag{20a}$$

$$n_d^A = 2n_d^0 - n - \chi n_p + \left(\chi + 1\right) n_p^0 - \left(\psi - 1\right) n_\psi \tag{20b}$$

$$n_m = 2n - \left(\chi + 2\right) n_p^0 + \chi n_p - 2n_d^0 + \left(\psi - 2\right) n_\psi \tag{20c}$$

$$\rightarrow n_d = n_d^A + n_d^B = 2n_d^0 - n - \left(\chi + 1\right) n_p + \left(\chi + 2\right) n_p^0 - \left(\psi - 1\right) n_\psi \tag{20d}$$

Introducing $\xi = \dfrac{n_p^0}{n_d^0}$ $\rightarrow$ $n_d^0 = \dfrac{n^0}{(1+\xi)}$, $n_p^0 = \dfrac{n^0 \xi}{(1+\xi)}$ and taking into account that $n = Zn^0$, Eqs. (20) become:

$$n_m = 2Zn^0 - \frac{(\chi+2)\xi+2}{(1+\xi)}n^0 + \chi n_p + (\psi-2)n_\psi \tag{21}$$

$$n_d = \frac{(\chi+2)\xi+2}{(1+\xi)}n^0 - Zn^0 - (\chi+1)n_p - (\psi-1)n_\psi \tag{22}$$

Recalling that (assuming the vibrational degree of freedom to be frozen) the specific heat at constant volume and constant pressure reads:

$$C_v = \hat{R}\left[\frac{3}{2}n_m + \frac{5}{2}n_d + 3\left(n_p + n_\psi\right)\right] \tag{23a}$$

$$C_p = C_v + R_{gas} = C_v + ZR_0 \tag{23b}$$

Substituting eqs .(21) and (22) into eq. (23a), one gets

$$C_v = \hat{R}\left\{\frac{n^0 Z}{2} + n^0\left[\frac{(\chi+2)\xi+2}{(1+\xi)}\right] + n_p\left(\frac{1}{2}-\chi\right) + \left(\frac{5}{2}-\psi\right)n_\psi\right\} \tag{24}$$

Introducing the molar fractions as $n_p^* = \frac{n_p}{n} \rightarrow n_p = n_p^* n = n_p^* Z n^0$ and $n_\psi^* = \frac{n_\psi}{n} \rightarrow n_\psi = n_\psi^* n = n_\psi^* Z n^0$, the constant γ can be expressed as:

$$\gamma = \frac{\frac{3}{2}Z + \left[\frac{(\chi+2)\xi+2}{(1+\xi)}\right] + n_p^* Z\left(\frac{1}{2}-\chi\right) + n_\psi^* Z\left(\frac{5}{2}-\psi\right)}{\frac{1}{2}Z + \left[\frac{(\chi+2)\xi+2}{(1+\xi)}\right] + n_p^* Z\left(\frac{1}{2}-\chi\right) + n_\psi^* Z\left(\frac{5}{2}-\psi\right)} \tag{25}$$

Moreover, recalling that $\xi = \frac{n_p^0}{n_d^0}$, the following relationships can be readily obtained:

$$\left(n_p^0\right)^* = \frac{n_p^0}{n^0} = \frac{n_p^0}{n_p^0 + n_d^0} = \frac{\xi}{\xi + 1} \tag{26a}$$

$$\xi = \frac{\left(n_p^0\right)^*}{1 - \left(n_p^0\right)^*} \tag{26b}$$

$$\text{and} \left[\frac{(\chi + 2)\xi + 2}{(1 + \xi)}\right] = \left[\chi\left(n_p^0\right)^* + 2\right] \tag{26c}$$

and γ can finally be re-cast in compact form as:

$$\gamma = \frac{3Z + 4 + \zeta}{Z + 4 + \zeta} \tag{27a}$$

$$\zeta = 2\chi\left[\left(n_p^0\right)^* - n_p^* Z\right] + n_p^* Z + n_\psi^* Z(5 - 2\psi) \tag{27b}$$

where $\left(n_p^0\right)^*$ is the molar fraction of the polyatomic species (e.g. CO_2 or CH_4 depending on the considered mixture) in the reference state (initial conditions with completely combined gas) and n_p^* the corresponding molar fraction in the equilibrium state; moreover, n_ψ^* account for the molar fraction of the new polyatomic species formed by monoatomic species (HNC).

As the reader will readily verify, for an initial mixture formed by diatomic gases only ($\left(n_p^0\right)^* = \eta_p^* = n_\psi^* = 0 \rightarrow$ ζ=0), the above formula reduces to the classical expression elaborated by Vincenti and Kruger [23], i.e.

$$\gamma_{VK} = \frac{3Z + 4}{Z + 4} \tag{28}$$

D. Centerline Total Enthalpy Measurements

Having finished the description of the modelling hierarchy used to extend the original Vincenti and Kruger's expressions to the case of initial mixtures of N_2 and CO_2 or CH_4 (which should be regarded as the necessary theoretical foundation for a well-posed application of the frozen sonic flow method to these mixtures), we now turn to discussing alternate techniques, which can be used to obtain independent estimates of the centerline enthalpy.

1. Heating Rate Method (HRM)

With the so-called Heating Rate Method (HRM), the stream enthalpy can be determined from measurements of the heating rate and pressure at the stagnation point of a blunt model placed at the stream centerline in the framework of the Goulard-Pope theory. Indeed, this method has its root in the studies by Goulard [30], who considered the stagnation-region convective heat transfer in chemically frozen boundary layers (a situation very akin to that established inside the SPES). For a hemispherical or near-hemispherical nose, the ratio of the heating rate at a partially catalytic surface to the heating rate at a fully catalytic surface is (Pope [31]):

$$q\sqrt{\frac{R}{p_{02}}} = KH_{cl}\left[1-\frac{\left(Le^{2/3}\alpha_e\dfrac{h_d^0}{H_{cl}}\right)}{1+\left(Le^{2/3}-1\right)\alpha_e\dfrac{h_d^0}{H_{cl}}}\right]\left(1-\varphi\right) \tag{29a}$$

with

$$\varphi = \left\{1+\frac{0.665T_w}{Sc^{2/3}k_w}\left(\frac{Z_eR_0\mu_e}{RP_{02}T_em_0}\right)^{1/2}\left[2\left(H_{cl}-\alpha_eh_d^0\right)\frac{\rho_\infty}{\rho_e}\left(2-\frac{\rho_\infty}{\rho_e}\right)^{1/4}\right]\right\}^{-1} \tag{29b}$$

(for the meaning of symbols and related units, see the related list**,** the constant K can be evaluated as K = 0.0323 + 0.00233 m_0 where m_0 is the molecular mass of the un-dissociated gas, Sutton and Graves [32]). As the reader

will easily realize, application of eq. (29) requires availability of some quantities ($\alpha_e, Z_e, \mu_e, k_w, T_w, T_e, \frac{\rho_\infty}{\rho_e}$), which, in practice, are still evaluated in the framework of the FSFM method presented in Sect. III.B, while the Lewis and Schmidt numbers can be assumed to be of unit order of magnitude (in particular, following Pope [31], we have used Le=0.9 and Sc=0.5, respectively). Also, T_w was set to 400 [K] for all tests.

For $k_w = \infty$ (fully catalytic surface), eq. (29) reduces to the well-known Zoby formula (Zoby [33]):

$$q_{fc} = KH_{cl}\sqrt{\frac{p_{02}}{R}} \tag{30}$$

For $k_w = 0$ (non-catalytic surface), eq. (29) reduces to:

$$q\sqrt{\frac{R}{p_{02}}} = KH_{cl}\left[1-\frac{\left(Le^{2/3}\alpha_e\frac{h_d^0}{H_{cl}}\right)}{1+\left(Le^{2/3}-1\right)\alpha_e\frac{h_d^0}{H_{cl}}}\right] \tag{31}$$

The precise assessment of the catalytic gas-surface interaction is generally regarded as very complex issue. Proper understanding of this phenomenon calls for very complex modelling at the molecular level, which can only be partly validated in ground-based plasmatron facilities (Garcia et al. [34]). As in the absence of experimental data (no information available for the specific gas mixtures considered in the present work), the use of models is the only possible alternative, here the values of the constant k_w for each gas mixture are determined using the formula based on the Maxwellian velocity distribution. Though this formula does not take into account concentration gradients due to catalysis, it has enjoyed a widespread use in the literature because it aligns with Goulard's main assumption of a frozen boundary layer (Goulard [30]; Cheung et al. [35,36]):

$$k_w = \eta_w\sqrt{\frac{R_0 T_w}{2\pi m_0}} \tag{32}$$

where η_w is the catalytic efficiency (i.e. the fraction of atoms that recombine upon striking the wall), and T_w the wall temperature (400 K). For the case of copper, relevant information on the recombination of hydrogen can be

found in the paper by Wood and Wise [37], while a big amount of data relating to nitrogen, oxygen and air has been summarized in [35,36]. As pure copper is nearly fully catalytic in all cases (see Table 1 in [36] and Table I in [37]), we assume $\eta_w = 0.1$ for all gas mixtures; to ensure this condition, at each heat-flux shot the surface calorimeter was cleaned by ethyl alcohol. The corresponding values of k_w are 13.75 for pure N_2, 13.51 for N_2 - O_2, 12.82 for N_2 - CO_2, 14.41 for N_2 - CH_4.

Heat fluxes were measured by a hemispherical probe, 9.2 mm ext. dia, equipped with a slug sensor having a full scale of $2x10^4$ kW/m^2; the impact pressure at the stream centerline, p_{02}, was measured using a water-cooled, stainless steel Pitot probe having the same nose geometry of the heat flux probe, connected to a capacitive absolute pressure transducer.

2. Calorimetric Probe Method (CPM)

With this alternate method, the centerline stream enthalpy is evaluated directly using a calorimetric probe as shown in Fig. 3; the complete probe assembly is composed of a water-cooled-stainless steel probe, a closed loop cooling water circuit, a gas sampling line, and a data acquisition and control unit.

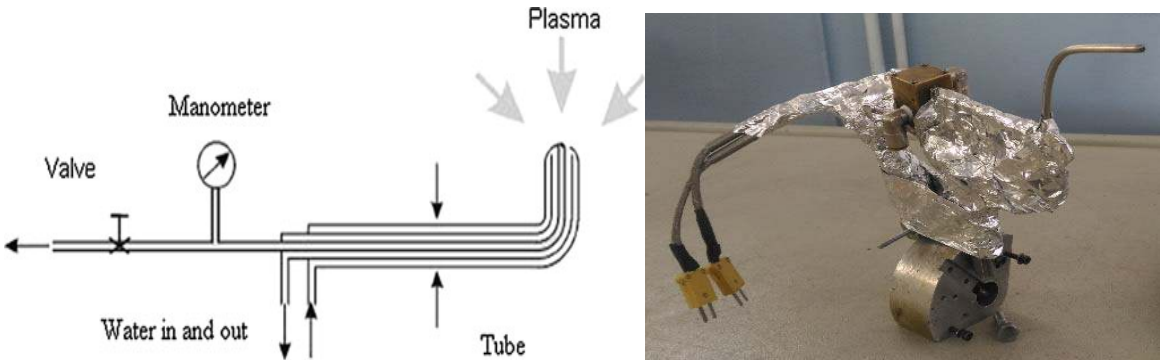

Figure 3: Total enthalpy probe: a) Sketch, b) picture.

Each measurement was accomplished in two successive steps; the first step is a 'tare' measurement of the heat load to the probe in the absence of gas flow through the probe. The second is a measurement of the heat load under 'flow' conditions (suction of a small amount of gas through the probe). By means of a combined energy balance, accounting for the cooling water flow through the probe and the gas sample extracted from the plasma, the local specific enthalpy at the probe tip can be calculated on the basis of a simple equation (Grey [38]), namely:

$$H_{cl} = Cp_g T_g + \frac{\left(m_{H2O} Cp_{H2O} \Delta T_{H2O}\right)_{flow} - \left(m_{H2O} Cp_{H2O} \Delta T_{H2O}\right)_{tare}}{m_g} \tag{33}$$

where $(\Delta T_{H2O})_{flow}$ and $(\Delta T_{H2O})_{tare}$ are the cooling water temperature jumps during tare and flow phases, m_{H2O} is the water mass flow rate, Cp_{H2O} is the water specific heat, Cp_g and T_g are the specific heat and temperature of the gas at the probe exit; moreover

$$m_g = \left[F(\gamma) p_0 A^*\right] / \sqrt{RT_0} \tag{34}$$

is the extracted gas sample, where $F(\gamma)$ comes from Eq.(6), p_o and T_o are the pressure and temperature upstream the throat of sonic nozzle, A* is the throat area and R is the gas constant.

It is possible to define a sensitivity factor, to relate the heat transferred from the plasma to the probe-cooling water via the following equation:

$$\sigma = \frac{\left(\Delta T_{H2O}\right)_{flow} - \left(\Delta T_{H2O}\right)_{tare}}{\left(\Delta T_{H2O}\right)_{flow}} \tag{35}$$

If a too low gas quantity is sampled, $(\Delta T_{H2O})_{flow}$ will be very small compared to $(\Delta T_{H2O})_{tare}$, leading to a large uncertainty for the measured enthalpy. On the contrary, if a too large gas quantity is sampled, the flow will be very disturbed near the probe tip, leading to large errors on the measured enthalpy. We assumed that this factor had to be greater than 5% to achieve an acceptable accuracy of thermocouples (in other words, this means making sure that supply of heat from the gas sampling is sufficient in comparison to the total heat transfer to the probe).

The used probe was AISI 316 stainless-steel made with a tip curved to right angle to protect the remaining probe parts from the hot gas, outer diameter 4 mm, and diameter of the sampling tube 1.2 mm.

IV. Results and Discussion

A. Pure Nitrogen: Effect of Different Factors on the Centerline Enthalpy Peaking

As explained to a certain extent in the introduction, the ratio of the center-line to bulk enthalpy can display sensitivity to different factors, some of geometrical nature, other of fluid-dynamic nature, which can make this ratio very dependent on the specific situation considered (thereby hindering investigators' efforts to make their results general and widely applicable to different situations). For this reason, we deemed it necessary to conduct a preliminary study aimed to determine quantitatively the impact of such factors on the quantity of interest, i.e. the H_{cl}/H_N ratio determined with the Frozen Sonic Flow Method.

For simplicity (to filter out the effect of other parameters), we have concentrated on the case of pure nitrogen as plasma gas, as reported in detail in the following.

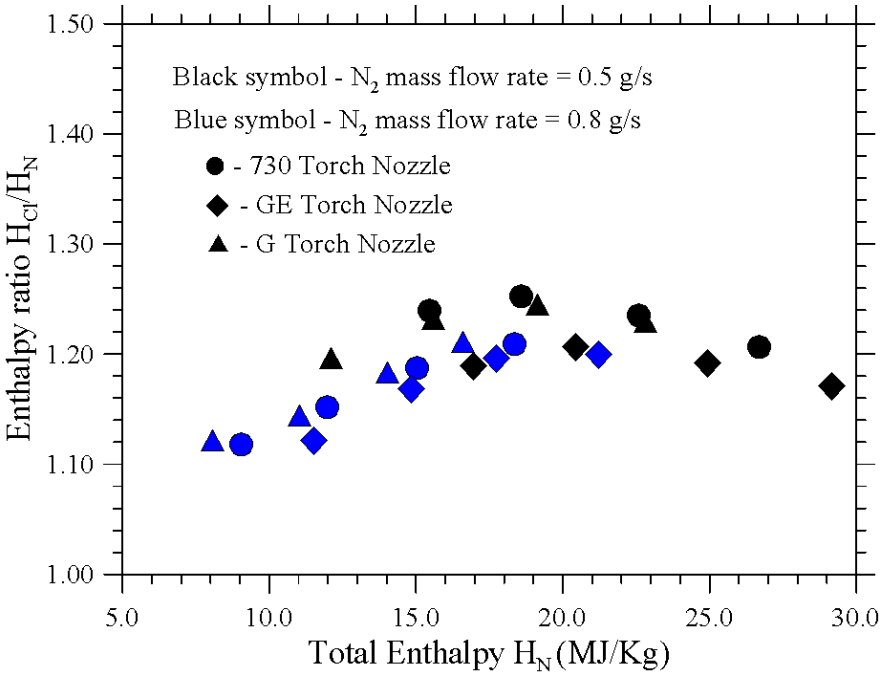

Figure 4. H_{cl}/H_N ratio for different torch nozzles (GE, G, 730)

a) physical geometry of the heater: in our heater (industrial plasma torch, Sulzer-Metco 9-MB, with arc swirl stabilization), the only allowed geometry variations are those obtainable by varying the anode (nozzle); we used three nozzles suitable for nitrogen, called 730, GE and G respectively (all nozzle types have a convergent section followed by a short cylindrical section, but only the 730 type ends with a slightly divergent section). The H_{cl}/H_N ratio is shown in Fig. 4 as function of the bulk enthalpy H_N using the three aforementioned torch nozzles

for two distinct mass flow rates (0.5 and 0.8 g/s respectively); as the reader will easily realize by inspecting this figure, the ratio is almost constant.

b) geometry of mixing chamber: the mixing chamber geometry is cylindrical (22 mm dia) but two length are possible, 46 and 103.7 mm, leading to L/D = 2.09 – 2.95 - 4.71 (the reader being referred to Figure 5 for the outcomes of the related tests).

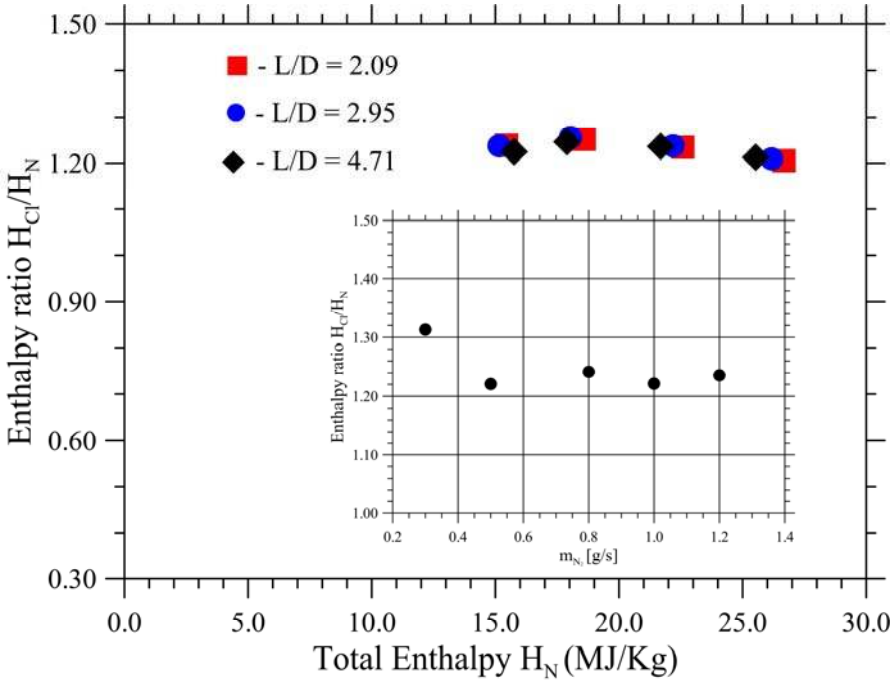

Figure 5. H_{cl}/H_N ratio for different L/D ratios, nozzle 730 and mass flow rate = 0.5 g/s (the insert shows H_{cl}/H_N ratio for different mass flow rates and L/D = 2.09)

c) gas mass flow rate : the insert in Figure 5 refers to a large number of tests performed with five Nitrogen mass flow rates (0.3 - 0.5 - 0.8 -1 - 1.2 g/s) . The ratio H_{cl}/H_N is practically the same for all tests.

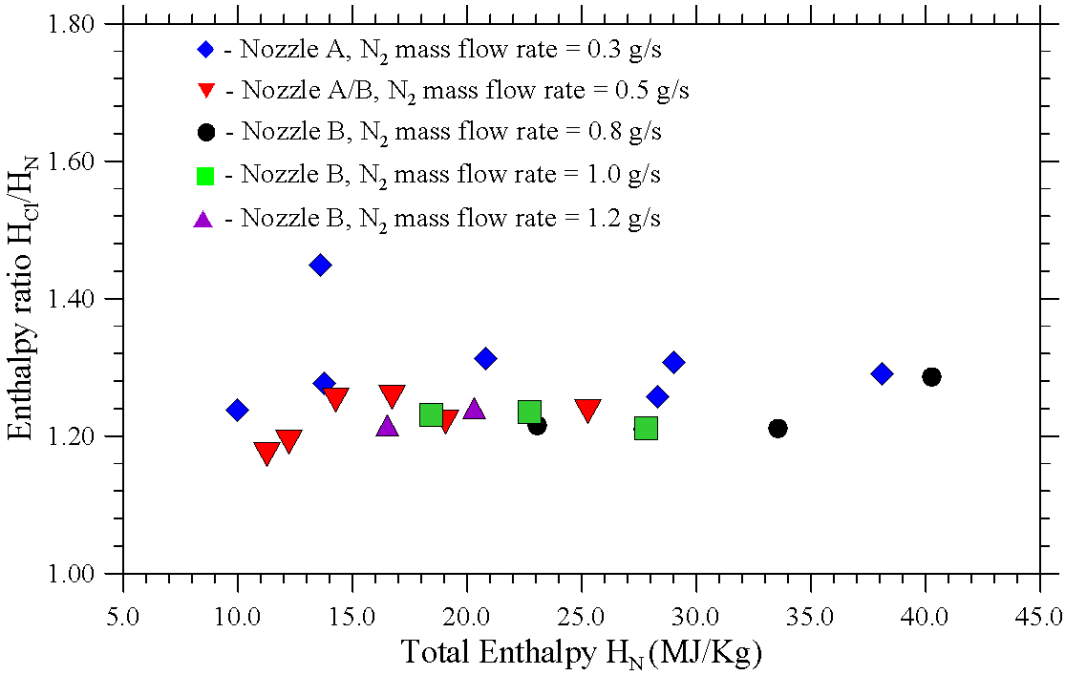

Figure 6. H_{cl}/H_N ratio for different nozzles.

d) nozzle configuration: Figure 6 summarizes the results for two different nozzles (area ratio 56 and 4, named "A" and "B", respectively). The ratio H_{cl}/H_N is practically the same for all tests.

On the basis of these preliminary results, it can, therefore, be concluded that the examined factors have a scarce effect on the measured ratio. This result is not completely unexpected. Assuming an experimental setup similar to the present one, other investigators came to similar conclusions [15].

B. Centerline Enthalpy by Frozen Sonic Flow Method

All the findings described in this section have been obtained using the following configuration for SPES: Arc-heater: nozzle 730, Mixing Chamber: L/D = 2.09, Supersonic Nozzle, A/ A* = 2.94, exit nozzle diameter: 22 (mm).

1. Pure Nitrogen and Air (reference Cases)

In this section we concentrate on the very classical case represented by a mixture of nitrogen and oxygen, namely, air. As in this case both component gases satisfy the original assumptions on which the Vincenti and Kruger's formula is based (initial diatomic and symmetrical gases only), the application of the FSFM approach

reduces to its standard implementation (Z and γ computed according to eqs. (9) and (28), respectively). The related results are summarized in Figs. 7-9.

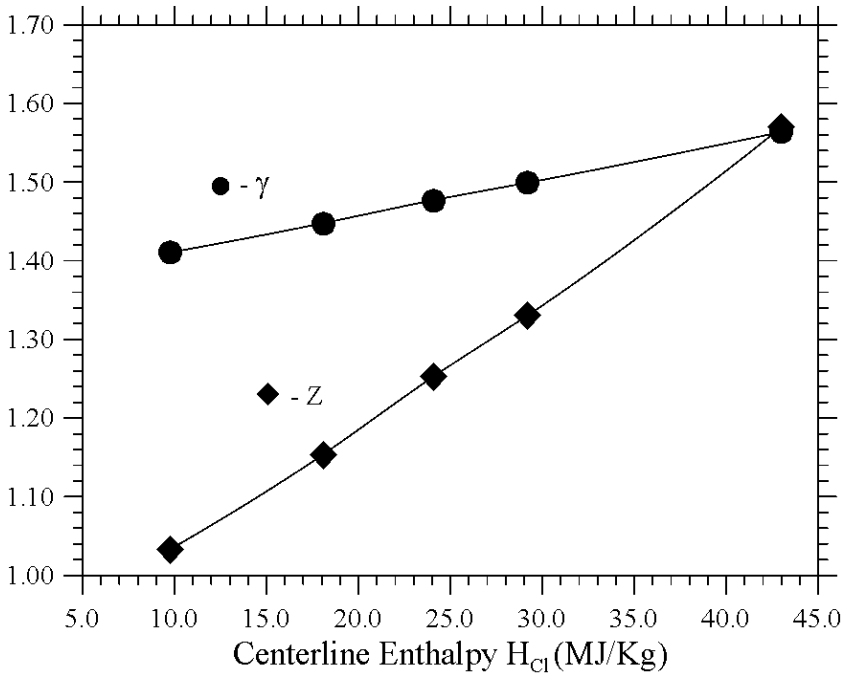

Figure 7 : Pure Nitrogen

More precisely, while Fig. 7 still referes to the case of pure nitrogen (showing how the related Z and γ parameters change as a function of the centerlien enthalpy, Fig. 8 illustrates the variation of the same quantities for the case of air, thereby giving insights into the effect produced by the addition of oxygen.

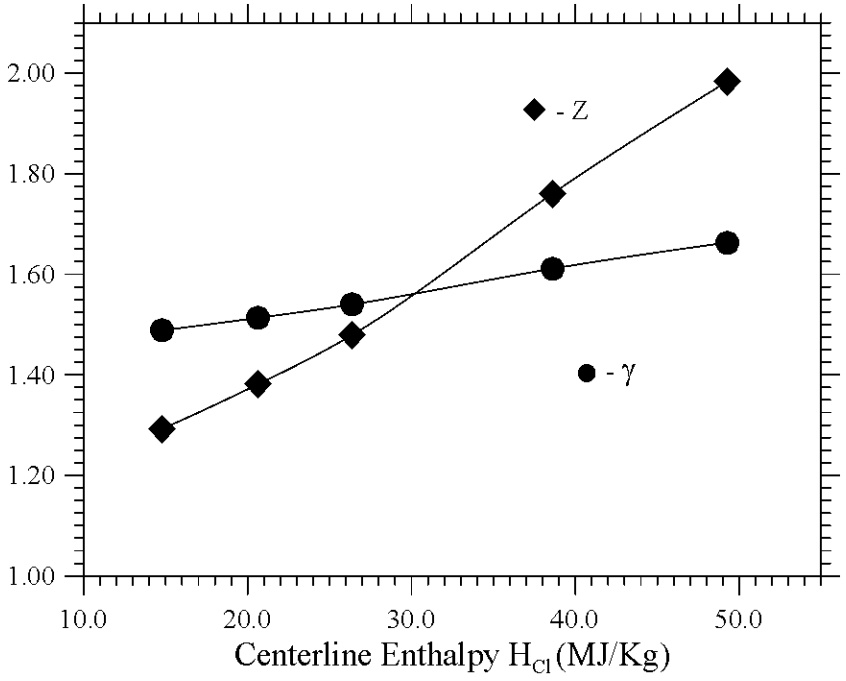

Figure 8. Air (Nitrogen-Oxygen Mixture)

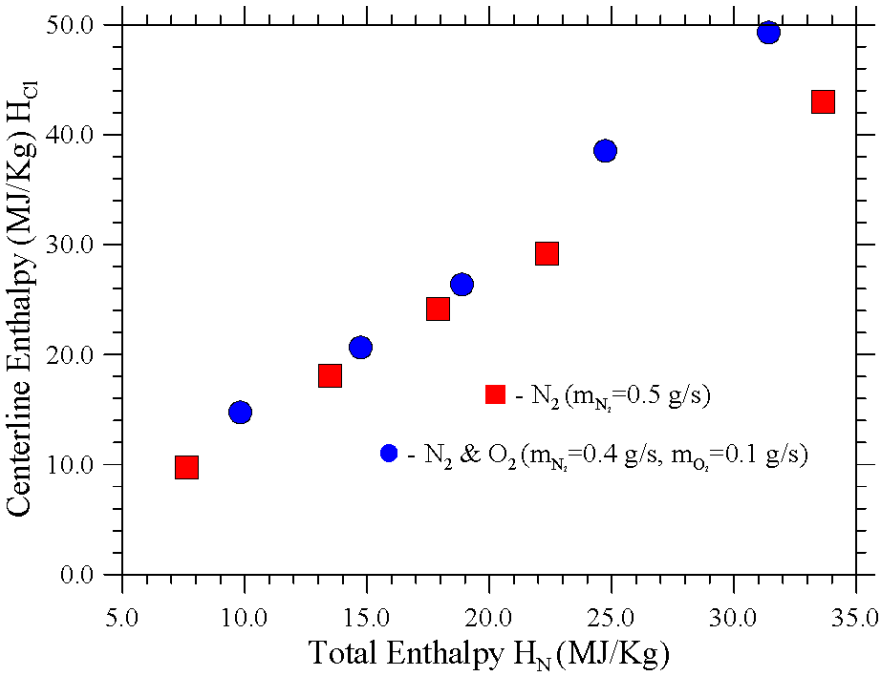

Figure 9. Pure Nitrogen – Air (nitrogen-oxygen mixture)

Figure 9 shows for both cases of pure nitrogen and air the variation of the centerline enthalpy as a function of the total enthalpy. It can be seen that while for relatively small values of the total enthalpy (H_N<20 MJ/Kg) the scattered points are quite well aligned along a line with constant inclination (regardless of whether they relate to pure nitrogen or air), some appreciable difference can be spotted according to the considered gas or mixture when this threshold is exceeded.

2. Nitrogen-Carbon Dioxide Mixture

The presence of Carbon Dioxide in the mixture formally invalidates eqs. (9) and (28), which have to be replaced with the corresponding corrected (expanded) versions, represented by eqs. (10) and (27), respectively.

Interestingly, the results summarized in Fig. 10 indicate that the differences between the values obtained with the correct version of the expressions of Z and γ and those obtained pretending that the considered gases are diatomic and symmetric (Z_{VK} and γ_{VK}) are relatively limited. More precisely, Z_{VK} and γ_{VK} slightly overestimate the corresponding values yielded by eqs. (10) and (27), respectively. This trend is reverted when the ratio Hcl/H_N is considered (Fig. 10c).

This scenario can easily be interpreted considering the nature of the CO_2 molecule, which by simply dissociating in CO and O, can cause a limited departure from the idealized behavior originally theorized by Vincenti and Kruger [23] (formalized by eqs. (9) and (28)).

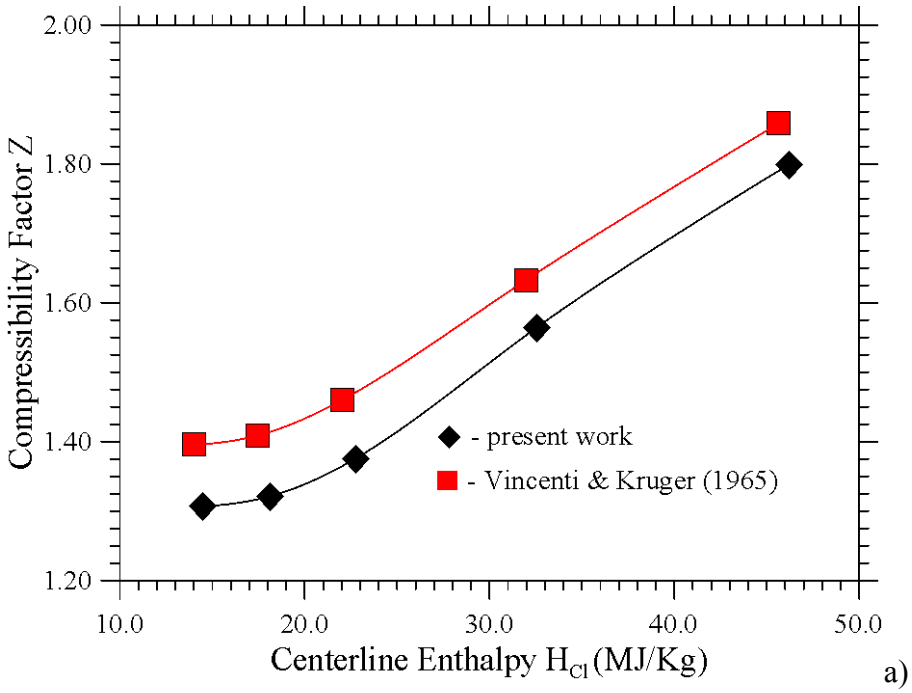
2.00
1.80
1.60
1.40
1.20
Compressibility Factor Z
10.0
20.0
30.0
40.0
50.0
Centerline Enthalpy H_{Cl} (MJ/Kg)
- present work
- Vincenti & Kruger (1965)

a)

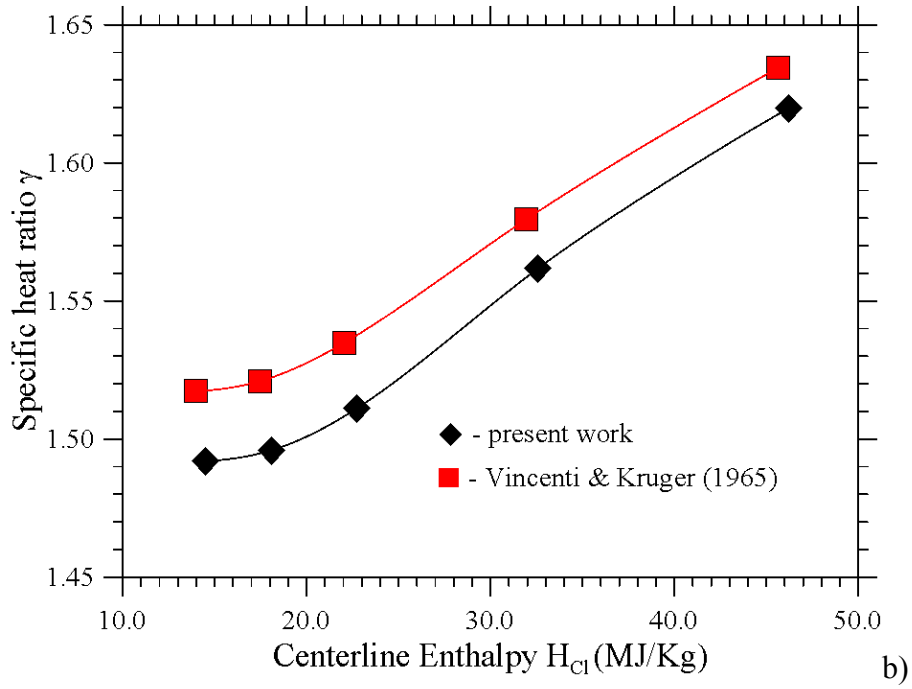
1.65
1.60
1.55
1.50
1.45
Specific heat ratio γ
10.0
20.0
30.0
40.0
50.0
Centerline Enthalpy H_{Cl} (MJ/Kg)
- present work
- Vincenti & Kruger (1965)

b)

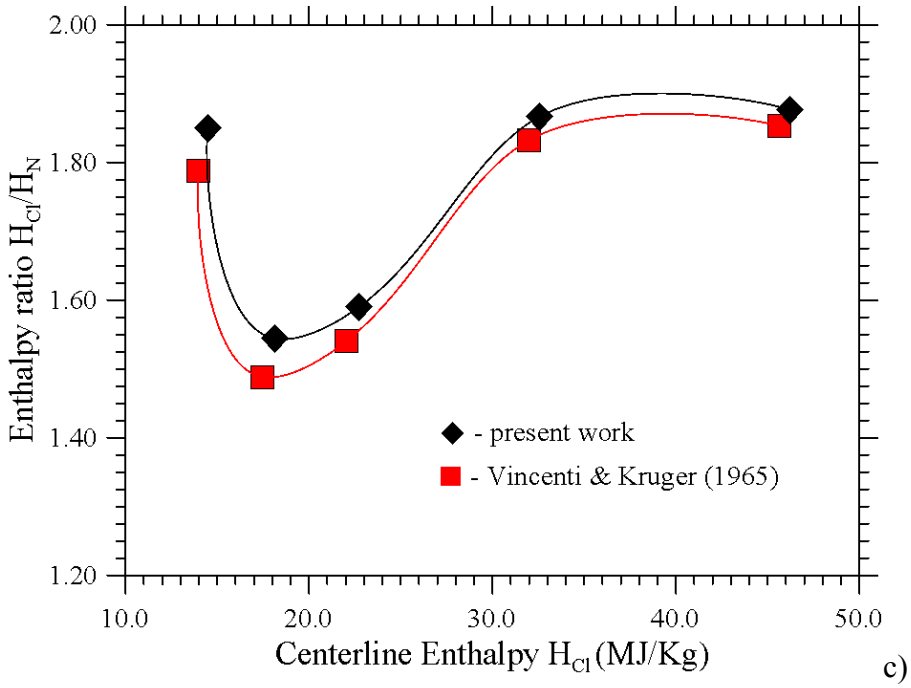

Figure 10. Nitrogen-Carbon Dioxide Mixture: a) Z as a function of centerline enthalpy, b) γ as a function of centerline enthalpy, c) Hcl/H_N as a function of centerline enthalpy.

3. Nitrogen-Methane Mixture

The same descriptive approach undertaken in Sect. IV.B.2 is replicated in this section by replacing the carbon dioxide with methane (i.e. a mixture of N_2 and CH_4), see Fig. 11.

It can be seen now that the differences between the results provided by the corrected formulas and those valid for diatomic and symmetric gases become significant. While Z computed with eq. (9) varies (approximately) in the range $1.2<Z_{VK}<1.4$, the corresponding value yielded by eq. (10) spans the interval $1.6<Z<2.5$. Similarly for the isentropic exponent, the related intervals are (approximately) $1.45<\gamma_{VK}<1.55$ and, $1.6<\gamma<1.8$ respectively.

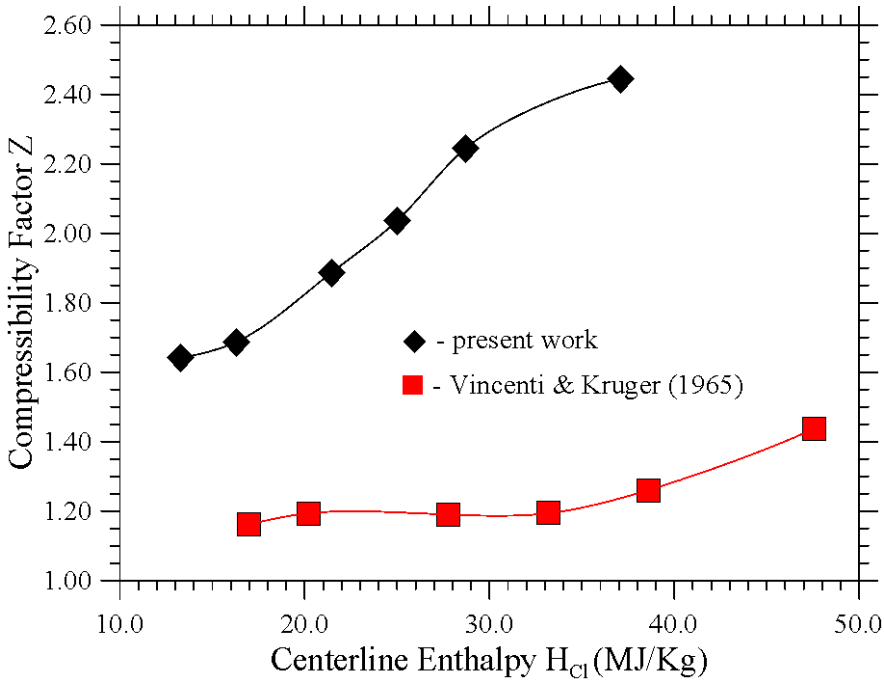
Compressibility Factor Z
2.60
2.40
2.20
2.00
1.80
1.60
1.40
1.20
1.00
10.0
20.0
30.0
40.0
50.0
Centerline Enthalpy H_{Cl} (MJ/Kg)
- present work
- Vincenti & Kruger (1965)

a)

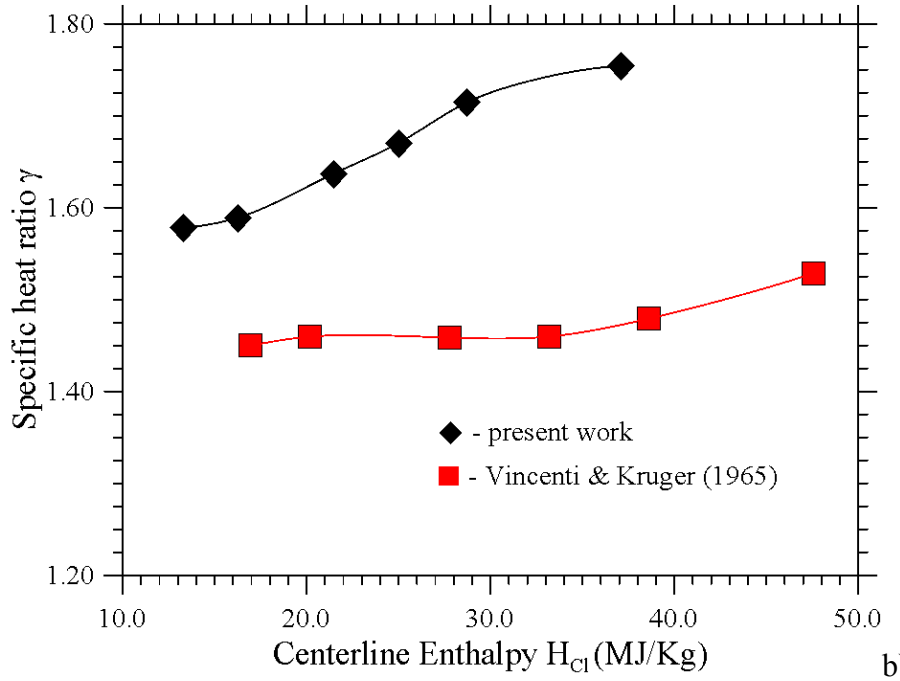
Specific heat ratio γ
1.80
1.60
1.40
1.20
10.0
20.0
30.0
40.0
50.0
Centerline Enthalpy H_{Cl} (MJ/Kg)
- present work
- Vincenti & Kruger (1965)

b)

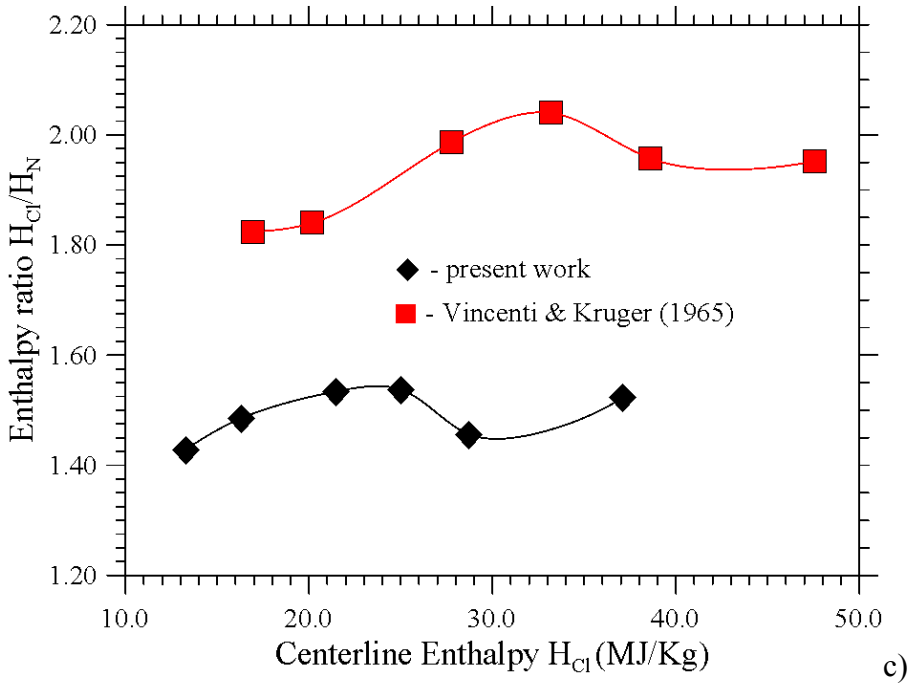

Figure 11: Nitrogen-Methane Mixture: a) Z as a function of centerline enthalpy, b) γ as a function of centerline enthalpy, c) Hcl/H_N as a function of centerline enthalpy.

These significant changes can obviously be ascribed to the much more involved situation that is established when methane is considered. When its molecule dissociates in the presence of atomic nitrogen, it leads to the formation of new tri-atomic species, which persist in the final state. The interplay of diatomic and monoatomic species and their evolution through the dissociation stage is also much more complex than that occurring for a mixture of nitrogen and carbon dioxide.

C. Centerline Enthalpy by Heating Rate Method

Toward the ultimate goal of using the FSFM approach to address the challenges described in the introduction, it is extremely important that it is validated and verified. Given the intrinsically complex nature of the considered problems, in particular, we have implemented such a process via two distinct stages of verification. As shown in the following, first we will compare the results obtained with the FSFM with the independent values yielded by the Heating Rate Method (present section) and then try to gain further confidence in the validity of the approach resorting to the Calorimetric Probe Method (Sect. IV.D).

Obviously, critical information about the reliability of the overall theoretical-experimental framework is sought from consideration of the four different archetypal situations examined so far (namely, pure nitrogen, air, nitrogen-carbon dioxide and nitrogen-methane mixtures).

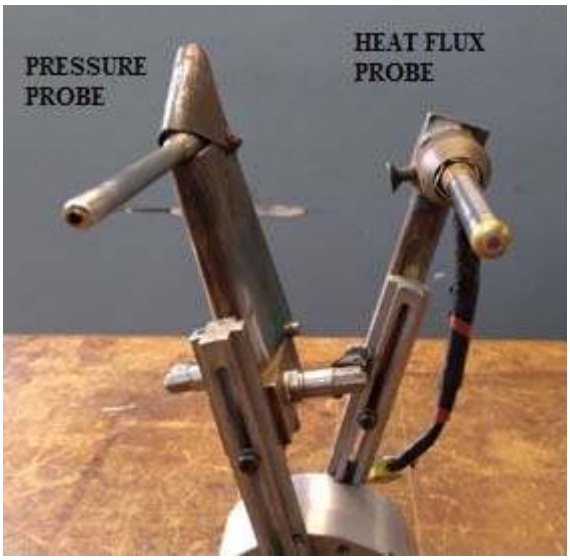

Figure 12. the probes used to apply the Heating Rate Method

The probes used to apply the Heating Rate Method are shown in Fig. 12.

1. Pure Nitrogen and Air (Reference Cases)

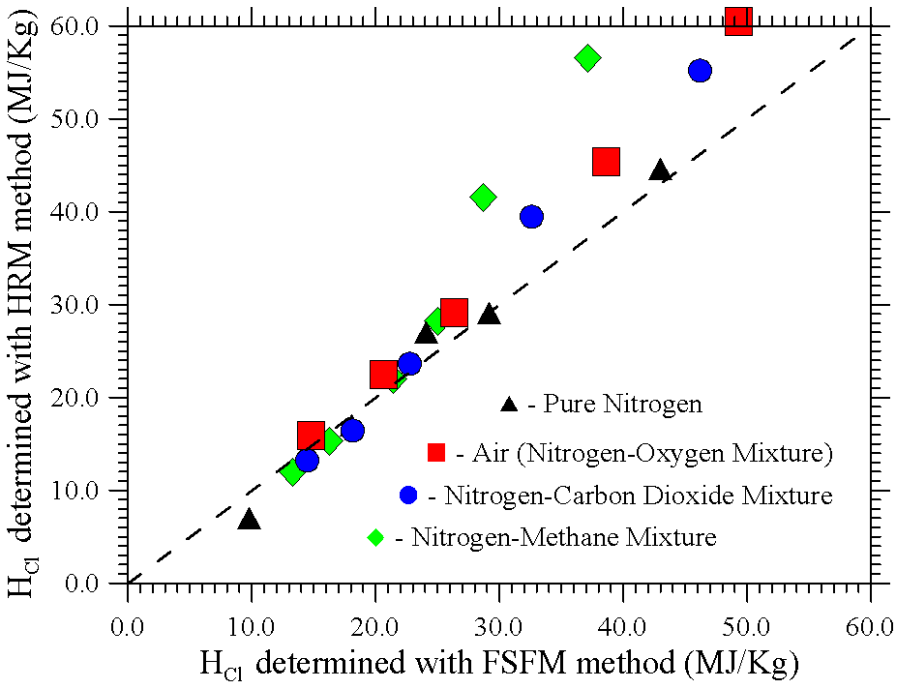

Figure 13. Comparison of centerline enthalpy determined with the FSFM and HRM methods.

As evident in Fig. 13, the agreement in the case of pure nitrogen is excellent, whereas some appreciable departure of the experimental points from the ideal $H_{HR}=H_{FSFM}$ straight line can be seen for the case of air. We

ascribe the later effect to a possible uncertainty in the estimated catalicity (the k_w constant appearing in Sect. III.D.1) of the body surface and/or in the chemical composition of the mixture after the dissociation process.

2. Nitrogen-Carbon Dioxide Mixture

The very good agreement seen for the case of pure nitrogen is back when the mixture of nitrogen and carbon dioxide is considered (Fig. 13).

3. Nitrogen-Methane Mixture

The data in Figure 13 for the case of the N_2-CH_4 mixture finally conclude the set of scheduled cross comparisons between the outcomes of the FSFM and HRM methods. The agreement holds provided the enthalpy does not exceed a limiting value of approximately 25 MJ/Kg. Above this threshold a clear departure of the experimental points from the ideal straight line can be identified, which we ascribe once again to the unavoidable uncertainties in the chemical composition of the mixture and the effective degree of catalysis of the involved surfaces required for the correct application of the method described in Sect. III.D.1.

Table 1: Comparison between the FSFM, HRM and CPM methods.

Mixture	H_N	FSFM	HRM	CPM
N_2	19.4	23.9	23.7	26.3
N_2-O_2	15.1	20.8	23.5	21.8
N_2-CO_2	18.2	21	20.4	22.5
N_2-CH_4	17.3	22.9	24.6	24.9

D. Centerline Enthalpy by Calorimetric Probe Method

In this section, we finally complement the earlier findings with dedicated measurements performed using the Calorimetric Probe Method (Fig. 14). Given the extreme complexity relating to such tests, we concentrate on a single (representative) case for each gas mixture, as reported in Table 1:

Figure 14. Calorimetric Probe Method: a) setup, b) snapshot of the jet, nitrogen-carbon dioxide mixture, c) snapshot of the jet, nitrogen-methane mixture.

1. Pure Nitrogen and Air (reference Cases)

As usual, first we consider the two reference cases relating to pure nitrogen and air. As witnessed by the data collected in Table 1, the agreement can be considered more than satisfactory.

The value provided by the CPM (H_{CPM} = 26.3 MJ/kg) slightly overestimates the values obtained with the FSFM and HRM methods in the case of pure nitrogen. For the mixture of nitrogen and oxygen, H_{CPM} takes an intermediate value with respect to those yielded by the FSFM and CPM (H_{CPM} = 21.8 MJ/kg).

2. Nitrogen-Carbon Dioxide Mixture (Gamma from present analysis)

For the mixture of nitrogen and carbon dioxide, the values provided by FSFM and HRM are very similar, with the CPM method slightly overestimating the other two results (H_{CPM} = 22.5 MJ/kg, Table 1).

3. Nitrogen-Methane Mixture (Gamma from present analysis)

The agreement is still good when the most complex case is considered, i.e. the mixture of nitrogen and methane (H_{CPM} = 24.9 MJ/kg). In this case, apparently the FSFM method provides a value that is slightly smaller than the values obtained with the HRM and CPM methods.

We wish to expressly point out at this stage, that the minor differences highlighted so far must obviously be ascribed to the unavoidable experimental errors, the limited knowledge about the values to be used for the catalysis constant k_w related to the HRM method, and, last but not least, the uncertainties relating to the effective chemical composition of the mixture after the decomposition process (resulting in 10-15% total uncertainty for the CPM and 20-25% for the HRM).

Leaving aside for a while, the many factors which might have contributed to determine such minor differences, there is compelling evidence that the results provided by different methods are in agreement.

The consistency of the FSFM predictions with experimental data obtained following alternate strategies suggests that physics-controlling steps have been taken into account, and that simplifications or assumptions introduced in the implementation of all these methods do not distort actual behavior.

We wish also to recall that, for the case of air, the ratio Hcl/H_N is almost equal to that obtained by Park et al. [19], which may indicate inherent similarities in the experimental apparatus and setup used by these authors and in the present work. Unfortunately, to the best of our knowledge, for the mixtures of nitrogen and carbon-dioxide or methane, no results exist in the literature with which direct comparison could be considered (which provides further rationale to our decision to tackle the problem in the framework of a multi-method approach).

V. Conclusion

The present work should be regarded as quite an exhaustive attempt to help engineers, researchers and professionals working in the field of thermal protection systems to discern the complex interrelations among the various parameters under one's control (that are not independent of one another) and to elaborate rational

guidelines relating to approaches that can influence the probability of success in measuring reliable values of the centerline enthalpy.

We have shown that different methods and approaches exist, whose nature and variety may implicitly suggest a concerted strategy of analysis based on the combination of existing theories on the behavior and evolution of gases, the tools of statistical physics, thermodynamics, fluid dynamics, nonlinear dynamics, and mathematical modeling in synergy with experimentally oriented work.

From the experimental point of view, by means of a Small Plasma Entry Simulator (SPES) and using Nitrogen (N_2) as hot feeding gas, three mixtures have been investigated by adding cold gases - oxygen (O_2), carbon dioxide (CO_2) and methane (CH_4) - through a mixer located just upstream the nozzle. The bulk enthalpies have been varied in the range between 5 and 30 [MJ/kg].

From a theoretical point of view, as in the final states of the N_2-CO_2 and the N_2-CH_4 atmospheres linear tri-atomic molecules, namely CO_2 and Hydrogen Cyanide (HCN) are present that can obviously make not rigorously applicable the classical formulation of the Frozen Sonic Flow Method, an attempt has been made to derive a theoretical formulation of compressibility factor Z and specific heats ratio γ for a mixture of monoatomic, diatomic and linear tri-atomic molecules with frozen vibrational energy.

The results obtained by the FSM modified in such a way have been compared with experimental ones obtained in the framework of alternate techniques, namely, the Heating Rate Method, based on measurements of the stagnation-point heat flux and impact pressure and relying on the well-assessed Goulard-Pope theory on heat transfer on catalytic surfaces, and the Calorimetric Probe Method, based on direct localized measurements of the enthalpy. The agreement has been found to be good (with minor differences due to unavoidable experimental uncertainties), leading to the following enthalpy ratios (averaged values obtained considering the results of the three different methods considered in the present work): H_{cl}/H_{ne} =1.46 for N_2-O_2 mixture, H_{cl}/H_{ne} = 1.17 for N_2-CO_2 mixture and H_{cl}/H_{ne} = 1.39 for N_2-CH_4 mixture.

We think that the most important outcomes of the present efforts relate to the clear indication they provide about the possibility to overcome typical experimental difficulties (which often hamper physicists' and engineers' quest to map precisely the response of these systems in the space of parameters) by using a complementary set of techniques. Quantities determined with one method can be substituted into the equations or relationships governing other methods, which, in turn, can feed back, other information for further iterative refinement of them or improvements in the underlying theoretical models (along these lines, as an example, we plan to devote other effort in the future to further investigate the idiosyncrasy that apparently affects the results obtained with

the HRM method when an enthalpy of 25 MJ/Kg is exceeded). We sincerely hope that the results and ideas presented in this work will be collected by other investigators and help them to produce further progress in these fields.

Acknowledgements

The authors would like to thank F. Aponte for the kind support provided during the execution of the experiments.

References

[01] De Filippis F., Purpura C., Viviani A., Acampora L., and Fusco M., (2010), "Chemical Species and Nonequilibrium Temperatures for Airflows in a Plasma Wind Tunnel", *Journal of Thermophysics and Heat Transfer,* 24(2), 271-280. DOI: 10.2514/1.43050

[02] De Filippis F., Delvecchio A., Viviani A., Cantiello I., Natale M., and Di Costa M., (2008), "Spectroscopic Analysis of Non-Equilibrium Air Jet in the Plasma Wind Tunnel SCIROCCO", 46th AIAA Aerospace Sciences Meeting and Exhibit, Aerospace Sciences Meetings, DOI: 10.2514/6.2008-1275

[03] Zare-Behtash H., Kontis K., Gongora-Orozco N., Takayama K., (2010), "Shock wave-induced vortex loops emanating from nozzles with singular corners", *Experiments in Fluids*, 49(5), 100. DOI 10.1007/s00348-010-0839-7

[04] Zare-Behtash, H., Lo, K.H., Yang, L., Kontis, K., (2016), "Pressure sensitive paint measurements at high Mach numbers", *Flow Measurement and Instrumentation*, 52, 10-16. DOI: 10.1016/j.flowmeasinst.2016.02.004

[05] Balboni J.A., (2015), "Consolidating NASA's Arc Jets", Book Publisher: NASA.

[06] Esposito A., Monti R., Russo G.P., Savino R., Ferrigno F., (1997), "Upgrading of an arc-heated flow facility for re-entry simulation", Proceedings of the 1997 8th International Conference on Computational Methods and Experimental Measurements (ISSN: 1369734X), CMEM; Rhodes, Greece; ; 1 May 1997 through 1 May 1997; Code 46674, Pages 491-500.

[07] Esposito A., De Rosa F., Filippis F., Graps E., Trifoni E., (2009), "A new concept of heat-flux probe for the Scirocco plasma wind tunnel", 16th AIAA/DLR/DGLR International Space Planes and Hypersonic Systems and Technologies Conference; Bremen; Germany; 19 October 2009 through 22 October 2009; Code 81964, article number 2009-7245. DOI: 10.2514/6.2009-7445

[08] Zuppardi G. and Esposito A., (2001), "Blowdown arc facility for low-density hypersonic wind-tunnel testing", *Journal of Spacecraft and Rockets*, 38(6), 946-948. DOI: 10.2514/2.3769

[09] Zuppardi G. and Esposito A., (2000), "Recasting the Fay-Riddell formulae for computing the stagnation point heat flux", Proceedings of the Institution of Mechanical Engineers, Part G: *Journal of Aerospace Engineering* 214(2), 115-120. DOI: 10.1243/0954410001531863

[10] Venkatapathy E., Laub B., Hartman G.J., Arnold J.O., Wright M.J., Allen G.A. Jr., (2009), "Thermal protection system development, testing, and qualification for atmospheric probes and sample return missions. Examples for Saturn, Titan and Stardust-type sample return", *Advances in Space Research* 44, 138–150. DOI: 10.1016/j.asr.2008.12.023

[11] Suess L.E, Milhoan J.D., Oelke L., Godfrey D. and Larin M.Y., Scott C.D., Grinstead J.H., Del Papa S., (2011), "Enthalpy Distributions of Arc Jet Flow Based on Measured Laser Induced Fluorescence, Heat Flux and Stagnation Pressure Distributions", JSC-CN-24062, 42nd AIAA Thermo-physics Conference; 27-30 Jun. 2011; Honolulu, HI; United States. DOI: 10.2514/6.2011-3778

[12] Winovich W., (1964), "On the equilibrium sonic-flow method for evaluating electric-arc air-heater performance", NASA TN D-2132.

[13] ASTM E341 -81 (reapproved 1992), "Standard Practice for Measuring Plasma Arc Gas Enthalpy by Energy Balance", https://www.astm.org/Standards/E341.htm

[14] Jorgensen L. H., (1964), "The total enthalpy of a one-dimensional nozzle flow with various gases", NASA TN D-2233 (1964)

[15] Pope R. B., (1968), "Measurements of enthalpy in low-density arc-heated flows", AIAA J., 6(1), 103-110. DOI: 10.2514/3.4448

[16] Hiester N. K. and Clark C. F., (1966), "Feasibility of Standard Evaluation Procedures for Ablation Materials", NASA CR-379.

[17] Zhang N., Sun F., Zhu L., Planche M.P., Liao H., Dong C., and Coddet C., (2012), "Measurement of Specific Enthalpy Under Very Low Pressure Plasma Spray Condition", *Journal of Thermal Spray Technology*, 21(3–4), 489–495. DOI: 10.1007/s11666-012-9738-1

[18] Scott C.D., (1993), "Survey of Measurements of Flow Properties in ArcJets", *J. Thermophys . Heat Transfer* 7, 9-24. DOI: 10.2514/3.11563

[19] Park C., Raiche G.A., Driver D.M., Olejniczak J., (2006), "Comparison of enthalpy determination methods for arc-jet facility", *J. Thermophysics and Heat Transfer*, 20(4), 672-678. DOI: 10.2514/1.15744

[20] Esposito A., Caso V. and Zuppardi G., (2014), "Upgrading the Frozen Sonic Flow Method for ArcJet Facilities", *J. Thermophysics and Heat Transfer*, 28(3), 565-567. DOI: 10.2514/1.T4321

[21] Lappa M., (2016), "A Mathematical and Numerical Framework for the Analysis of Compressible Thermal Convection in Gases at very high Temperatures", *Journal of Computational Physics*, 313, 687–712. DOI: 10.1016/j.jcp.2016.02.062

[22] Esposito A. and Aponte F., (2018), "Frozen Sonic Flow Method Applied to Arc-Heated Facilities for Planetary Re-Entry Simulation", *The Journal of Aerospace Science, Technology and Systems*, 97 (3), 153 -162. DOI: 10.1007/BF03404769

[23] Vincenti W.G. and Kruger C.H., (1965), "Introduction to Physical Gas Dynamics", John Wiley & Sons, New York, 1965.

[24] Chapman S. and Cowling T.G., (1970), "The Mathematical Theory of Non-Uniform Gases", 3rd edn., Cambridge University Press, London, 1970.

[25] Cheng, H. K. and Lee, R. S., (1966), "Freezing and Dissociation in supersonic nozzle flow", AIAA Paper 66-1. DOI: 10.2514/6.1966-1

[26] Brown S. C. "Basic Data of Plasma Physics", John Wiley and Sons, 1959, pp.318 -321

[27] Gross B., Grycz G. and Miklossi K. (1968), Plasma Technology, Iliffe Books Ltd London, 1968.

[28] Sanford G. and McBride B.J., (1994), "Computer Program for Calculation of Complex Chemical Equilibrium Compositions and Applications I. Analysis", NASA RP-1311, 1994

[29] Stull D.R. et al. "JANAF interim thermochemical Tables", The Dow Chemical Co., Midland, Mich. (Dec. 1960), see also www.kinetics.nist.gov/janaf/

[30] Goulard R., (1958), "On catalytic recombination rates in hypersonic stagnation heat transfer", Jet Propulsion 28, 737-745. DOI: 10.2514/8.7444

[31] Pope R. B., (1968), "Stagnation-Point Convective Heat Transfer in Frozen Boundary layers", AIAA J., 6(4), 619 -626. DOI: 10.2514/3.4554

[32] Sutton K. and Graves R.A., (1972), "A general stagnation-point convective heating equation for arbitrary gas mixtures", NASA TR R- 376.

[33] Zoby E., (1968), "Empirical Stagnation-Point Heat-transfer relation in Several Gas Mixtures at High Enthalpy Levels", NASA TN D-4799, 1968.

[34] García A., Chazot O. and Fletcher D., (2002), "Investigations in plasmatron facilities on catalycity determination", Proc. 4th Europ. Symp. Aerothermodynamics for Space Applications, 15-18 Oct., Italy, ESA SP-487, March 2002. Bib. Code 2002ESASP.487..489G

[35] Cheung T.M., Park G., and Schrijer F.F. J., (2015), "Oxygen and Nitrogen Surface Catalytic Recombination on Copper Oxide in Tertiary Gas Mixtures", The 2015 World Congress on Aeronautics, Nano, Bio, Robotics and Energy (ANBRE15), Incheon, Korea, August 25-28, 2015.

[36] Cheung T.M., Schrijer F.F.J., and Park G., (2016), "Nitrogen Catalytic Recombination on Copper Oxide in Tertiary Gas Mixtures", *Journal of Spacecraft and Rockets*, 53(4), 644-653. DOI: 10.2514/1.A33512

[37] Wood B.J and and Wise H., (1961), "Kinetics of hydrogen atom recombination on surfaces", *J. Phys. Chem*., 65 (11): 1976–1983. DOI: 10.1021/j100828a015

[38] Grey J., Jacobs P.F., Sherman M.P., (1963), "Calorimetric Probe for the Measurement of Extremely High Temperature", *Review of Scientific Instruments* , 34(8), 738 – 741.